Ground state properties of electron-hole bilayer: Mass-asymmetric effect

R. O. Sharma, L. K. Saini,* and Bhagwati Prasad Bahuguna

Applied Physics Department, Sardar Vallabhbhai National Institute of Technology, Surat 395007, Gujarat, India

(Received 6 May 2016; revised manuscript received 7 November 2016; published 28 November 2016)

We study the effects of mass asymmetry on the ground state properties of an electron-hole bilayer (EHBL) system at $T = 0$ by using the quantum Monte Carlo method. Particularly, we use the variational Monte Carlo method to calculate the pair-correlation function $g(r)$ and the condensation fraction c at a fixed density for different values of interplaner distance d and extract the phases of the EHBL system. We use a single trial wave function that can describe fluid, excitonic, and biexcitonic phases. We find that the excitonic fluid phase is stable in the region of $d \geqslant 0.25$ a.u. and a transition from the excitonic fluid phase to the biexcitonic fluid phase at $d = 0.24$ a.u.

DOI: 10.1103/PhysRevB.94.205435

I. INTRODUCTION

An electron-hole bilayer (EHBL) system, consisting of two spatially separated layers where electrons are confined to one layer and holes are in another, have attracted a lot of interest over the years in both theoretical [1–5] and experimental [6–10] levels. Such a system can be realized in double quantum well structures, e.g., GaAs/AlGaAs heterostructures and bilayer graphene with negligible tunneling between the two wells. The attractive Coulomb interaction between electrons and holes, confined in a different layer, starts to play an important role yielding a variety of interesting phenomena. In particular, the presence of excitonic and biexcitonic condensate phases [10–12], the charge-density wave phase [13–15], and enhanced critical density for the onset of Wigner crystals [16–18]. In the presence of strong perpendicular magnetic fields, fractional quantum Hall states [19,20] appear due to interlayer correlation effects. Coulombic interlayer friction (Coulomb drag) [2,8] influences the transport properties of double-layer systems. Due to these phases and promising applications in semiconductor devices, over the years, EHBL systems have considerable interest. Recently, Efimkin and Galitski [2] theoretically investigated the temperature dependence anomalous Coulomb effect in the GaAs/GaAlAs-based EHBL due to the formation of excitonic molecules. Berman *et al.* [3] used a BCS-like mean-field approximation to find the phase diagram of an *e*-*h* bilayer. Gamucci *et al.* [6] has experimentally shown a new class of heterostructure comprising single-layer graphene in proximity to a quantum well created in GaAs to study the Coulomb drag transport measurements. Matveeva and Giorgini [21] studied the BCS-BEC crossover in an EHBL system of fermionic dipoles and compared the results with mean-field theories.

The majorities of theoretical studies have considered the symmetric EHBL system where electrons and holes have equal masses to study the electronic correlation effects. Moreover, most of these theoretical studies were based on methods, such as dielectric formulations [13,22] and Bardeen-Cooper-Schrieffer theory [3,23], whereas very few groups have used the quantum Monte Carlo (QMC) method [16,24]. On the other hand, there are some studies on the mass-asymmetric EHBL that use the quantum Singwi-Tosi-Land-Sjölander [25] approach [15,26] and the path-integral Monte Carlo (PIMC) method [27,28], but here we use the variational quantum Monte Carlo (VMC) method. In literature, Ludwing *et al.* [28] have studied the effect of mass asymmetry on the Wigner crystallization. Later, Schleede *et al.* [27] have extended the work and completed the phase diagram of the mass-asymmetric EHBL for $d = 1$–100 a.u. using the PIMC method. In contrast to these works, we used the VMC method. In the present paper, we have considered the more realistic EHBL system with unequal masses of electrons and holes for the density range of $r_s < 10$ a.u. We have used a single trial wave function [24] that can describe the fluid phase, the excitonic phase, and the biexcitonic phase. The Wigner crystal phase, which is favorable at the very low-density (high-r_s) regime, is not considered in the present paper. In this paper, we found the biexcitonic phase at $r_s = 5$ a.u. for a hole-to-electron mass asymmetry of 7 (for the GaAs/GaAlAs-based system) which is stable against the excitonic fluid phase for $d \leqslant 0.24$ a.u. This biexcitonic fluid phase could not observed by Schleede *et al.* [27] as they have not considered $d < 1$ a.u.

II. MODEL

We consider an EHBL system consisting of two parallel two-dimensional layers separated by a distance d having electrons as carriers in one layer and holes in another. We also consider that the effective masses of electrons m_e^* and holes m_h^* are unequal, i.e., $m_e^* \neq m_h^*$. Hence, the layers are identical in each respect except for the charge and mass of the carriers. In the absence of the magnetic field, the Hamiltonian of the infinite EHBL system is given by

$$\hat{H} = -\frac{1}{2}\sum_i \nabla_{\mathbf{e}_i}^2 - \frac{1}{2\sigma}\sum_i \nabla_{\mathbf{h}_i}^2 + \sum_{i<j}\frac{1}{|\mathbf{e}_i - \mathbf{e}_j|} + \sum_{i<j}\frac{1}{|\mathbf{h}_i - \mathbf{h}_j|} - \sum_{i,j}\frac{1}{\sqrt{|\mathbf{e}_i - \mathbf{h}_j|^2 + d^2}}, \quad (1)$$

where $\mathbf{e}_i$ and $\mathbf{h}_j$ represent the coordinates of the ith electron and the jth hole, respectively, $\sigma = m_h^*/m_e^*$, and ϵ is the dielectric constant of the medium. Here, 1 Ha$^* = e^2/\epsilon a_B^*$, and the Bohr radius is $a_B^* = \epsilon\hbar^2/m_e^* e^2$ where ϵ is the dielectric constant of the medium. Since we have taken $m_e^* = 1$ and

*drlalitsaini75@gmail.com

$\epsilon = 1$, the modified units are the same as the atomic unit in the present calculations. To simulate an infinite system we use a finite square simulation cell with periodic boundary conditions and have used two-dimensional Ewald sums [29,30] to evaluate the Coulomb sums.

III. COMPUTATIONAL METHOD

We use the variational Monte Carlo (VMC) method as implemented in the CASINO code [31] in order to calculate various ground state properties of the EHBL system. In this method, the expectation value of the Hamiltonian $\hat{H}$ with respect to a trial wave-function Ψ_T is calculated using importance-sampled Monte Carlo integration. The trial wave function contains a number of variable parameters whose values are obtained by an optimization procedure. The VMC provides an upper bound for the exact ground state. The variational energy expectation value of $\hat{H}$ with trial wave-function Ψ_T is given by

$$\langle E_T \rangle = \frac{\int \Psi_T^*(\mathbf{R})\hat{H}\Psi_T(\mathbf{R})d\mathbf{R}}{\int \Psi_T^*(\mathbf{R})\Psi_T(\mathbf{R})d\mathbf{R}} = \int \frac{|\Psi_T(\mathbf{R})|^2}{\int |\Psi_T(\mathbf{R})|^2 d\mathbf{R}} E_L(\mathbf{R})d\mathbf{R}, \quad (2)$$

where $\mathbf{R} = (r_1, r_2, \ldots, r_N)$ is all particle positions and $E_L(\mathbf{R}) = \Psi_T^{-1}(\mathbf{R})\hat{H}\Psi_T(\mathbf{R})$ is the local energy.

We use a trial wave function of the standard Slater-Jastrow type,

$$\Psi_T = D[\phi(\mathbf{e}_i^{\uparrow} - \mathbf{h}_j^{\downarrow})]D[\phi(\mathbf{e}_i^{\downarrow} - \mathbf{h}_j^{\uparrow})]\exp[J(\mathbf{R})], \quad (3)$$

where Ds are Slater determinants of opposite-spin electron-hole pairing orbitals and $\exp[J(R)]$ is a Jastrow factor, introducing the correlation between the charge carriers. We have used the pairing orbitals from Ref. [24],

$$\phi(\mathbf{r}) = \sum_{l=1}^{n_p} p_l \cos(\mathbf{k}_l \cdot \mathbf{r}) + f(r; M) \sum_{m=0}^{n_c} c_m r^m, \quad (4)$$

where n_p is the plane-wave expansion order, $\mathbf{k}_l$ is the lth shortest reciprocal-space vector, n_c is the polynomial expansion order, $f(r; M)$ is a cutoff function given by $f(r; M) = (1 - r/M)^3\Theta(r - M)$, Θ is the Heaviside step function, and $\{p_l\}$, $\{c_m\}$, and M are optimizable parameters. The pairing orbitals implicitly bind the antiparallel spin electron-hole pairs, hence it is capable of describing a pure Fermi fluid and an excitonic superfluid but cannot describe the biexcitons. The biexciton correlations are introduced by the Jastrow factor.

We have used a CASINO's Jastrow factor [32] consisting of a two-body polynomial u term to which the electron-electron, hole-hole, and electron-hole Kato cusp conditions are applied [33]. Also, we have used a "quasicusp" Jastrow factor term [24] Q to include the electron-hole cusp condition as $d \to 0$ except for $d = 0$. The Q term has a single optimizable cutoff length. We have optimized the parameters of a trial wave function using minimization of the mean absolute deviation of the local energies from the median [31] followed by linear least-squares energy minimization [34].

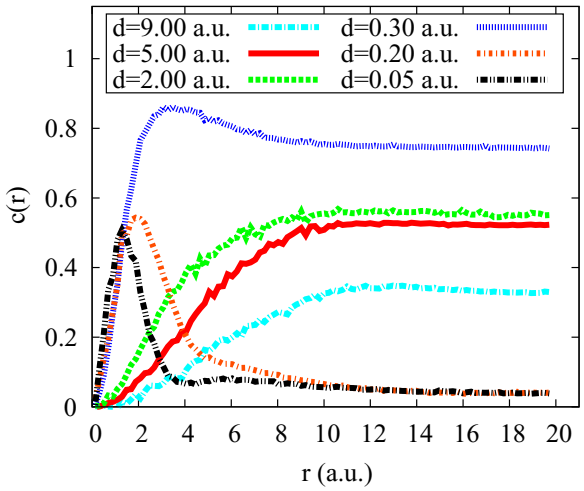

FIG. 1. VMC expectation values of $c(r)$ for the EHBL bilayer at $d = 9$, 5, 2, 0.3, 0.2, and 0.05 a.u. for $r_s = 5$ a.u. and $m_h = 7 \times m_e$.

The translational-rotational average of the two-body density matrix for electron-hole pairs is

$$\rho_{eh}^{(2)}(r) = \frac{N^2 \int |\Psi(\mathbf{R})|^2 \frac{\Psi(\mathbf{e}_1+\mathbf{r}', \mathbf{h}_1+\mathbf{r}')}{\Psi(\mathbf{e}_1, \mathbf{h}_1)} \delta(|\mathbf{r}'| - r)d\mathbf{R}\, d\mathbf{r}'}{\Omega^2 2\pi r \int |\Psi(\mathbf{R})|^2 d\mathbf{R}}, \quad (5)$$

where Ω is the area of the simulation cell. The condensate fraction c is defined as [35]

$$c = \frac{\Omega^2}{N} \lim_{r\to\infty} \rho_{eh}^{(2)}(r). \quad (6)$$

The condensate fraction is evaluated by using the improved estimator of Ref. [36], which is denoted as $c(r)$ in Fig. 1. Within the QMC calculations, we have evaluated the condensate fraction c by fitting the $c(r)$ over the plateau region [16] with $c + A/r^2$, $r \geqslant 10$ for large r. The condensate fraction is zero for pure one-component and biexcitonic fluid phases. We

TABLE I. Extrapolated condensate fraction c and ground state energy per particle of the EHBL system within the VMC calculation at a density of $r_s = 5$ a.u. and different layer separations d.

d (a.u.)	c	Energy (a.u./particle)
9.00	0.330(2)	− 0.10668(4)
7.00	0.403(2)	− 0.10914(4)
5.00	0.524(1)	− 0.11528(4)
2.00	0.550(1)	− 0.14321(5)
1.70	0.765(1)	− 0.16770(3)
1.00	0.7955(6)	− 0.21653(4)
0.50	0.745(1)	− 0.2972(1)
0.40	0.741(1)	− 0.3329(1)
0.30	0.7401(6)	− 0.3828(1)
0.26	0.739(2)	− 0.4084(1)
0.25	0.8394(3)	− 0.42462(9)
0.24	0.0856(6)	− 0.4258(1)
0.20	0.0290(9)	− 0.4574(2)
0.10	0.0322(6)	− 0.6054(1)
0.05	0.0318(5)	− 0.7263(3)
0.04	0.007(1)	− 0.7654(3)

compute the pair-correlation function (PCF) to distinguish the biexcitonic fluid phase from the one-component fluid phase.

The spherically averaged real-space PCF [24] is given by

$$g_{\alpha\beta}(r) = \frac{\Omega \int |\Psi(\mathbf{R})|^2 \delta(\mathbf{r}_\alpha - \mathbf{r}_\beta - \mathbf{r}')\delta(|\mathbf{r}'| - r) d\mathbf{R}\, d\mathbf{r}'}{2\pi r \int |\Psi(\mathbf{R})|^2 d\mathbf{R}}, \quad (7)$$

where α and β are indices that distinguish the four particle types in the system, i.e., up- and down-spin electrons and holes. The PCF gives the probability of finding a particle at distance r away from a particle situated at the origin.

IV. RESULTS AND DISCUSSION

In this section, we present the numerical results for the ground state properties of the EHBL system with mass asymmetry. The results were obtained by the VMC simulation method as implemented in the CASINO code [31]. The ground

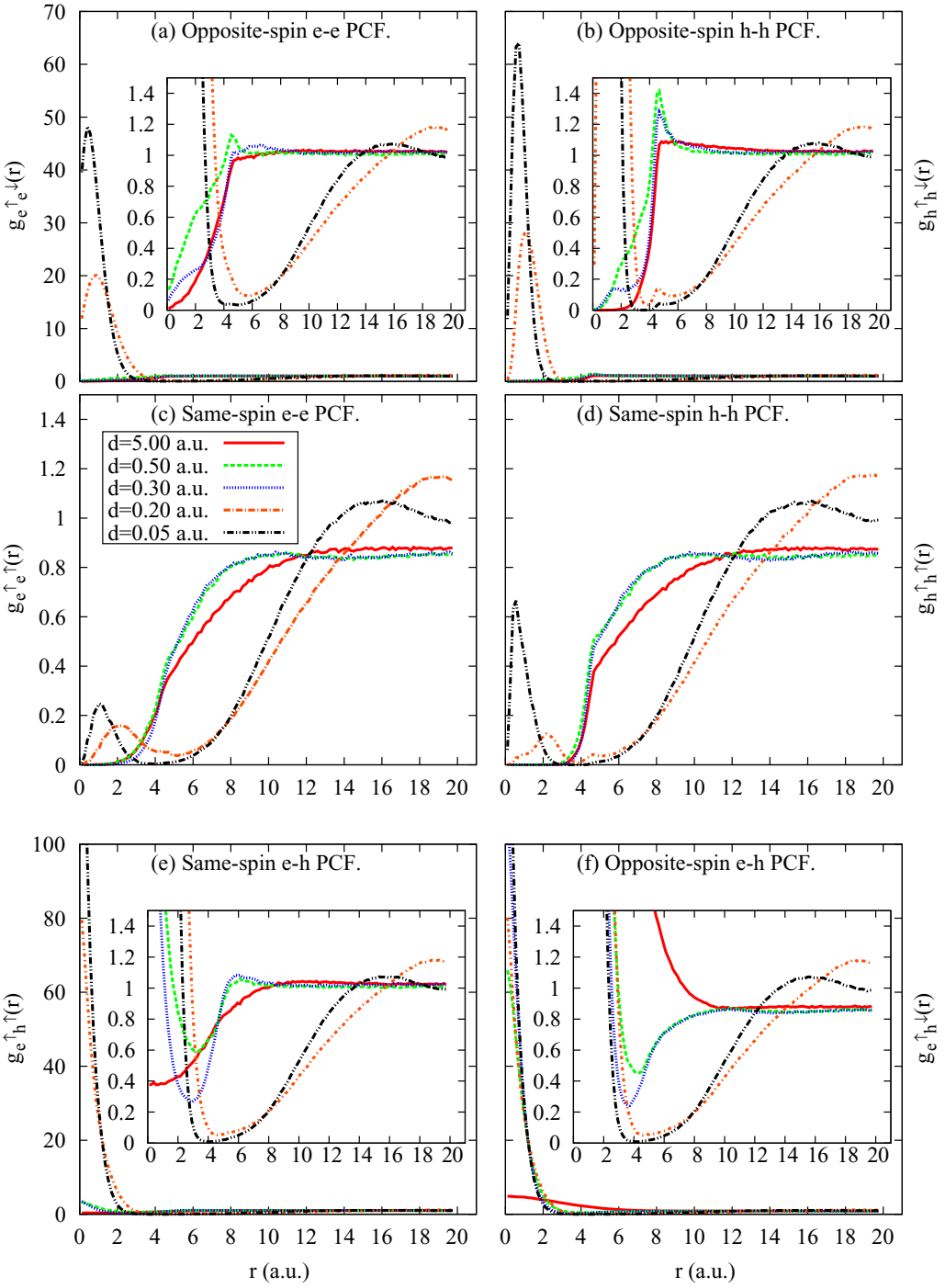

FIG. 2. Intralayer PCF, (a) $g_{e\uparrow e\downarrow}$, (b) $g_{h\uparrow h\downarrow}$, (c) $g_{e\uparrow e\uparrow}$, and (d) $g_{h\uparrow h\uparrow}$ and interlayer PCF, (e) $g_{e\uparrow h\uparrow}$ and (f) $g_{e\uparrow h\downarrow}$ for $d = 5$, 0.5, 0.3, 0.2, and 0.05 a.u. at $r_s = 5$ a.u. Up- ($\uparrow$) and down- ($\downarrow$) arrows represent up-spin and down-spin charge carriers, respectively. The legends are displayed in (c). The inset shows the zoomed view of the same data near the origin.

state properties of the EHBL system depend on the following parameters: (i) The hole-to-electron effective mass ratio $\sigma = m_h^*/m_e^*$, (ii) the interlayer separation d measures the interlayer coupling, and (iii) the density parameter r_s controls the in-layer coupling. In the simulations, we consider a bilayer system with $N = 5$ up- and down-spin electrons and holes, i.e., a total of 20 particles. Our results have been obtained at a fixed density parameter of $r_s = L/\sqrt{2\pi N} = 5$ a.u., where L is the side of the square simulation cell and mass ratio $\sigma = 7$ for different layer separations d.

Figure 1 displays the VMC computed values of $c(r)$ for the EHBL system with a density of $r_s = 5$ a.u. at interlayer separations $d = 9.0, 5.0, 2.0, 0.3, 0.2$, and 0.05 a.u. In the VMC simulation, $c(r)$'s were obtained by subtracting the one-body density matrix from the two-body density matrix [36]. It is noticed in Fig. 1 that $c(r)$ shows the plateau region at large r. The symmetric EHBL system studied by Maezono *et al.* [24] found $c(r) = 0$ at $r_s = 5$ and $d = 4$ a.u. indicates the system is in the fluid phase whereas in our case $c(r)$ is nonzero for $d = 5$ a.u. and increases with d. This difference can be interpreted as due to unequal masses of electrons and holes, residing in different layers, the mass-asymmetric EHBL is in the excitonic phase.

In Table I, we show the condensate fraction c and ground state energy per particle at different layer separations d. The condensate fraction c calculated by extrapolating [16] the $c(r)$ over the plateau region for large values of r with $c + A/r^2$, $r \geqslant 10$ [almost for all d's, $c(r)$ shows a plateau from $r = 10$ a.u.] at different values of d. The condensate fraction c is nonzero, and buildup as the separation between the layers decreases from $d = 9$ a.u. and achieves its maximum value of 0.8394(3) at $d = 0.25$ a.u. The nonzero values of the condensate fraction indicate that the EHBL system is in the excitonic fluid phase. By further diminishing the separation by 0.01 a.u., the condensate fraction suddenly falls to 0.0856(6), which is one order small and goes down by a further reduction in d. This can be interpreted as a phase transition from excitonic fluid to biexciton formation or the one-component fluid phase. So, in order to distinguish the biexcitonic phase from the one-component fluid, we have calculated the spin-resolved pair-correlation functions which are shown in Fig. 2.

The intralayer and the interlayer PCFs are shown in Figs. 2(a)–2(f), at layer separations $d = 5$, 0.5, 0.3, 0.2, and 0.05 a.u. The insets are shown in Figs. 2(a), 2(b), 2(e), and 2(f) that provide a zoomed view near the origin. It is evident, from an inspection of Figs. 2(a) and 2(b) (see the insets) and Figs. 2(c) and 2(d), that parallel spin (antiparallel spin) e-e/h-h PCF creates a Fermi hole (correlation hole) when layer separation is large, particularly at $d = 5, 0.5$, and 0.3 a.u. The Fermi hole for parallel spin e-e/h-h pairs is wider than the correlation hole for antiparallel e-e/h-h pairs. Whereas at the same values of d, the parallel and antiparallel spin e-h PCFs [Figs. 2(e) and 2(f)] at $r = 0$ show enhancement. This enhancement in the same- and opposite-spin e-h PCFs at $r = 0$ where the intralayer PCF is zero can be interpreted as a formation for excitons. By further diminishing the layer separation, the Fermi hole (correlation hole) for parallel (antiparallel) spin disappears and develops a peak near $r = 1$, see Figs. 2(a)–2(d). It is also evident that the peak height for

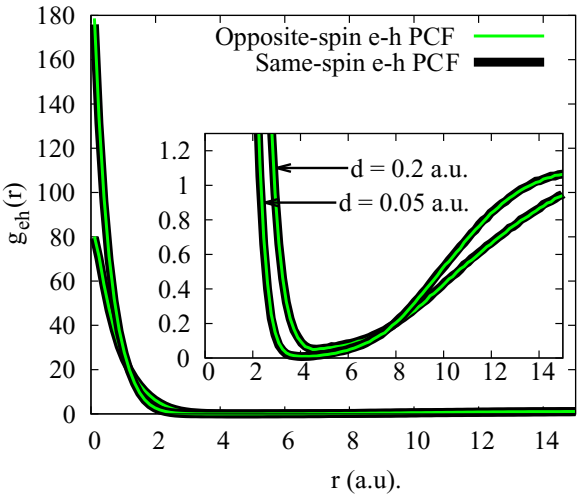

FIG. 3. The same- and opposite-spin e-h PCFs are shown as black-thick lines and green-thin lines (overlapped on the black-thick lines), respectively. The PCFs corresponding to the lower value at $r = 0$ a.u. is for $d = 0.2$ and that for the higher value is for $d = 0.05$ a.u. The inset shows the zoomed view of the same data near the origin.

h-h pair PCFs (for both parallel and antiparallel) is larger than the e-e pair PCFs that means the holes are comparatively more strongly correlated than the electrons. This can be interpreted as an effect of unequal masses of electrons and holes since the in-layer coupling parameter (the ratio of potential energy to kinetic energy) for the layer of holes is m_h^*/m_e^* times larger than the layer of electrons.

We also noticed from an inspection of Figs. 2(e) and 2(f) that, at $d = 5$–0.3 a.u. where the system is in an excitonic fluid, the same-spin e-h PCF at $r = 0$ remains close to zero whereas the opposite-spin e-h PCF builds up with d. This difference between two PCFs is due to the fact that our wave function explicitly binds opposite-spin electron-hole pairs. By further diminishing d to 0.2 a.u., the PCF shows a strong peak at $r = 0$ for both same- and opposite-spin e-h pairs, whereas opposite-spin e-e/h-h pairs show a fairly strong peak around $r = 1$ a.u. and same-spin e-e/h-h pairs show a small peak at $r \approx 2$ a.u. By further diminishing d to 0.05 a.u., peaks in the PCF enhanced more and also shifts towards the origin. For clarity, we compare the opposite- and same-spin e-h PCFs for $d = 0.2$ and 0.05 a.u. in Fig. 3. It is clear from an inspection of Fig. 3 that the same- and opposite-spin e-h PCFs at $r = 0$ are equally enhanced. This strong equal enhancement in the same- and opposite-spin e-h PCFs along with enhancement in the opposite-spin e-e/h-h PCF can be interpreted as a formation of a biexciton. The inset image shows the zoomed view around the origin, which shows that the PCF becomes zero around $r = 4$ a.u. for $d = 0.05$ a.u. and shows the weak oscillatory behavior at large r which can be interpreted as a biexcitonic fluid phase. The very small values of the condensate fraction, given in Table I, at $d \leqslant 0.24$ a.u. and the characteristics of the PCFs indicate that the mass-asymmetric EHBL system is in the biexcitonic fluid phase. We did not find the one-component fluid phase over the studied range which was reported in the study of the symmetric EHBL

by Maezone *et al.* [24] In contrast, we found an excitonic fluid phase at $d = 0.25$–9 a.u. for the mass-asymmetric e-h bilayer. In Ref. [24] the biexcitonic phase is observed for $d < 0.38$ a.u. whereas in the present case it is observed for $d \leqslant 0.24$ a.u. In our paper we found the biexcitonic phase at $r_s = 5$ a.u. for a hole-to-electron mass asymmetry of 7 (for the GaAs/GaAlAs-based system) which is stable against the excitonic fluid phase for $d < 0.25$ a.u. This biexcitonic fluid phase could not be observed by Schleede *et al.* [27] as they have not considered $d < 1$ a.u.

V. CONCLUSION

In conclusion, we have studied the effect of the unequal masses of electrons and holes on the ground state properties of the EHBL system. For this purpose, we have employed the VMC method over a wide range of layer parameters. The different phases of mass-asymmetric EHBL are identified from the behavior of the condensate fraction and pair-correlation functions at different layer separations. We find the excitonic fluid phase by a nonzero condensate fraction. We compute the PCF to identify the biexcitonic fluid phase from the one-component fluid phase. We found that the EHBL system is in the excitonic fluid phase when $d = 9$–0.25 a.u. and in the biexcitonic phase for $d < 0.25$ a.u. Here, we have not considered the low-density regime where the Wigner crystal phase is favorable nor the finite layer width effects. In the future, we will try to explore the phase diagram of the mass-asymmetric EHBL system for other values of r_s and will also include the finite width effect.

ACKNOWLEDGMENTS

One of the authors (R.O.S.) acknowledges the financial assistance provided by the Ministry of Human Resources and Development (MHRD), New Delhi, India. We wish to thank P. López Ríos and B. Tiwari for their fruitful discussions.

[1] K. Das Gupta, A. F. Croxall, J. Waldie, C. A. Nicoll, H. E. Beere, I. Farrer, D. A. Ritchie, and M. Pepper, Adv. Condens. Matter Phys. **2011**, 727958 (2011).
[2] D. K. Efimkin and V. Galitski, Phys. Rev. Lett. **116**, 046801 (2016).
[3] O. L. Berman, R. Y. Kezerashvili, and K. Ziegler, Physica E **71**, 7 (2015).
[4] Y. E. Lozovik and V. Yudson, JETP Lett. **22**, 274 (1975).
[5] Y. E. Lozovik, S. L. Ogarkov, and A. A. Sokolik, Phys. Rev. B **86**, 045429 (2012).
[6] A. Gamucci, D. Spirito, M. Carrega, B. Karmakar, A. Lombardo, M. Bruna, L. N. Pfeiffer, K. W. West, A. C. Ferrari, M. Polini, and V. Pellegrini, Nat. Commun. **5**, 5824 (2014).
[7] R. Pentcheva, M. Huijben, K. Otte, W. E. Pickett, J. E. Kleibeuker, J. Huijben, H. Boschker, D. Kockmann, W. Siemons, G. Koster, H. J. W. Zandvliet, G. Rijnders, D. H. A. Blank, H. Hilgenkamp, and A. Brinkman, Phys. Rev. Lett. **104**, 166804 (2010).
[8] A. Croxall, K. Das Gupta, C. Nicoll, I. Farrer, H. Beere, D. Ritchie, and M. Pepper, Physica E **42**, 1247 (2010).
[9] L. V. Butov, A. Imamoglu, K. L. Campman, and A. C. Gossard, J. Exp. Theor. Phys. **92**, 260 (2001).
[10] J. P. Cheng, J. Kono, B. D. McCombe, I. Lo, W. C. Mitchel, and C. E. Stutz, Phys. Rev. Lett. **74**, 450 (1995).
[11] V. B. Timofeev, A. V. Larionov, M. Grassi-Alessi, M. Capizzi, and J. M. Hvam, Phys. Rev. B **61**, 8420 (2000).
[12] R. M. Lee, N. D. Drummond, and R. J. Needs, Phys. Rev. B **79**, 125308 (2009).
[13] L. Liu, L. Świerkowski, D. Neilson, and J. Szymański, Phys. Rev. B **53**, 7923 (1996).
[14] L. Liu, L. Świerkowski, and D. Neilson, Physica B **249-251**, 594 (1998).
[15] R. K. Moudgil, J. Phys.: Condens. Matter **18**, 1285 (2006).
[16] S. De Palo, F. Rapisarda, and G. Senatore, Phys. Rev. Lett. **88**, 206401 (2002).
[17] R. K. Moudgil, G. Senatore, and L. K. Saini, Phys. Rev. B **66**, 205316 (2002).
[18] B. Tanatar and B. Davoudi, Phys. Rev. B **63**, 165328 (2001).
[19] Y. Shimoda, T. Nakajima, and A. Sawada, Physica E **22**, 56 (2004).
[20] Y. W. Suen, L. W. Engel, M. B. Santos, M. Shayegan, and D. C. Tsui, Phys. Rev. Lett. **68**, 1379 (1992).
[21] N. Matveeva and S. Giorgini, Phys. Rev. A **90**, 053620 (2014).
[22] J. Szymański, L. Świerkowski, and D. Neilson, Phys. Rev. B **50**, 11002 (1994).
[23] D. Neilson, A. Perali, and A. R. Hamilton, Phys. Rev. B **89**, 060502 (2014).
[24] R. Maezono, P. López Ríos, T. Ogawa, and R. J. Needs, Phys. Rev. Lett. **110**, 216407 (2013).
[25] T. Hasegawa and M. Shimizu, J. Phys. Soc. Jpn. **38**, 965 (1975).
[26] M. G. Nayak and L. K. Saini, Contrib. Plasma Phys. **52**, 211 (2012).
[27] J. Schleede, A. Filinov, M. Bonitz, and H. Fehske, Contrib. Plasma Phys. **52**, 819 (2012).
[28] P. Ludwig, A. Filinov, Y. E. Lozovik, H. Stolz, and M. Bonitz, Contrib. Plasma Phys. **47**, 335 (2007).
[29] D. Parry, Surf. Sci. **49**, 433 (1975).
[30] D. E. Parry, Surf. Sci. **54**, 195 (1976).
[31] R. J. Needs, M. D. Towler, N. D. Drummond, and P. López Ríos, J. Phys.: Condens. Matter **22**, 023201 (2010).
[32] N. D. Drummond, M. D. Towler, and R. J. Needs, Phys. Rev. B **70**, 235119 (2004).
[33] T. Kato, Commun. Pure Appl. Math. **10**, 151 (1957).
[34] C. J. Umrigar, J. Toulouse, C. Filippi, S. Sorella, and R. G. Hennig, Phys. Rev. Lett. **98**, 110201 (2007).
[35] C. N. Yang, Rev. Mod. Phys. **34**, 694 (1962).
[36] G. E. Astrakharchik, J. Boronat, J. Casulleras, and S. Giorgini, Phys. Rev. Lett. **95**, 230405 (2005).